Microarticle

Atomistic modeling of pileup process in metal deposition manufacture

Mehrdad Shahmohammadi Beni, Tzu Hsien Tan, K.N. Yu*

Department of Physics, City University of Hong Kong, Tat Chee Avenue, Kowloon Tong, Hong Kong

ABSTRACT

In present work, molecular dynamics (MD) simulation was employed to model the impact of single and double molten aluminum drops onto to an aluminum substrate. The study was related to the pileup process in metal deposition manufacture. Most previous investigations used the continuum scale Volume-of-Fluid (VOF) method to model this phenomenon. Here, the underlying mechanism of pileup process was examined in more details. The effect of impact speed on the height and width of the solidified drops was studied. The penetration depth of molten drops into the solid substrate was also investigated. The present model would be useful for future investigations as the process could now be studied at the atomic scale and the final solidified structure could also be assessed in terms of its defect and crystallinity.

Introduction

Metal microdroplet deposition has been exploited in the inject printing technology using molten metal to generate metallic three-dimensional (3D) parts. Such an additive manufacturing process has been desirable due to its relatively low cost and has attracted much interests in the past two decades [1–6]. However, problems were identified in the metal microdroplet deposition equipment due to poor metallurgical properties of the final structure as a result of bonding between the molten droplet and the substrate. To tackle these such problems, appropriate adjustment of parameters in the molten drop pileup process would be critical [7], which would in turn rely on understanding of the underlying mechanism. However, Wang et al. [8] commented that not much was known about the physical phenomena related to the pileup process such as molten drop spreading and generated shapes of solidified pileups, despite extensive studies on inkjet printing. Experimental studies on the pileup process in more details included those from Tsai et al. [9] and Son et al. [10]. On the other hand, computer simulations of the behavior pileup process employed the Volume-of-Fluid (VOF) method. For example, based on the VOF method, Du et al. [7] employed a continuum scale model to study a number of important parameters such as the capillary effect, as well as the bulk liquid and solidification mechanisms. Tian et al. [11] also made use of the continuum scale model to examine the impact of solder drops on a substrate. In relation, Li et al. [12] used the VOF technique to model the deposition of successive aluminum drops on a substrate and found that the aluminum drops solidified simultaneously as a result of heat transfer to the substrate. Notwithstanding the theoretical studies with continuum scale

simulations, detailed studies on the pileup process at the atomic scale would further reveal the underlying mechanism. In present work, molecular dynamics simulation was deployed to model the pileup process at the atomic scale.

Materials and methods

Molecular dynamics simulation was deployed to model the pileup process of molten aluminum drops on a flat solid aluminum substrate. In present work, three different potentials, namely embedded atom model (EAM) [13], modified embedded atom model (MEAM) [14] and charge-optimized many-body force field (Comb3FF) [15,16] for aluminum were adopted to describe the interaction between the aluminum atoms. The results from these three different interatomic potentials were compared.

As inspired by the previous work of Du et al. [7] using the continuum scale VOF model, two configurations were considered here, namely, (1) single and (2) double drop impact. The 3D modeled setup with dimensions is shown in Fig. 1. Here, a periodic simulation box was considered. The aluminum lattice was face centered cubic (FCC) with a lattice constant of 4.04. The diameter of the molten aluminum drop was assumed as 30 Å while the dimensions of the solid aluminum plate were taken as $100 \times 100 \times 30$ Å^3. The total number of atoms in the single (see Fig. 1a) and double drop (see Fig. 1b) cases were 1,288,670 and 1,345,113, respectively. The temperatures of the molten drop and the aluminum plate were set as 960 and 300 K, respectively. Initially, the system was relaxed under the constant number, volume and energy (NVE) ensemble for 10 ps, and the molten drop and aluminum plate
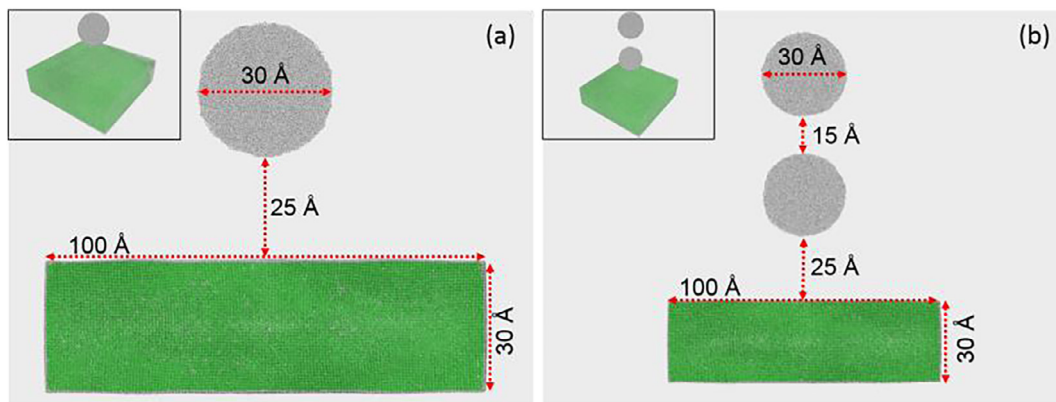

Fig. 1. Modeled configurations for (a) single and (b) double drop impact on a solid aluminum plate. (Grey color represents molten aluminum drop and green color represents the solid aluminum plate). (For interpretation of the references to color in this figure legend, the reader is referred to the web version of this article.)

were allowed to relax at their respective temperatures. Three different speeds at which the molten drop impacted onto the aluminum plate were studied, namely, 0.5, 1.0 and 2.0 Å/ps, under the constant number, volume and temperature (NVT) ensemble. The NVT ensemble performed time integration on Nose-Hoover thermostat [17] style non-Hamiltonian equations of motion which were designed to generate positions and velocities sampled from the canonical (i.e., NVT). This updated the position and velocity for atoms in the group in each time step. The time step was set to be 0.01 ps/step. After the molten drop impacted the surface of the aluminum plate, the system was allowed to relax at 300 K, the NVT ensemble was replaced by an NVE ensemble that updated the positions and velocities of the atoms. These settings enabled the atoms to interact more closely. During this process, energy was allowed to be transferred among atoms leading to conservation of the overall system energy. (Note: we employed similar technique and setting as used in the previous work of Shen et al. [18], where a molten nanosized gold droplet impacted the solid surface). At this stage, the temperatures of molten drop and plate were allowed to vary. This final relaxation stage lasted 200 ps for both cases of single and double molten drop.

In addition, the effect of surface roughness on the penetration depth of a single molten drop on the aluminum plate was investigated. Surface roughness was an important factor, as it was always present in aluminum plates in real experiments, at least on the nanoscale. To simplify the present task, we generated uniform sinusoidal roughness on top of the simulated aluminum plate. We used three different roughness values of 1, 3 and 6 Å, measured from the surface of the aluminum plate to the peak of the sinusoidally shaped surface roughness. The surface topology of aluminum plates with three different roughness values are shown in Fig. 2.

Results and discussion

Validation

To validate our model, we simulated a similar setup employed in the previous work of Shen et al. [18], where a molten gold drop impacted the surface of a gold substrate at an impact speed of 1 Å/ps and compared the results in Fig. 3(a), and the agreement was found to be good. In addition, we determined the temperature-dependent density of aluminum using our code and compared the results with those obtained experimentally that are being widely used in the material library of the commercial finite element method (FEM) codes. The data for the temperature-dependent material library was taken from the COMSOL Multiphysics commercial code. In our MD code, we modelled an aluminum block with 4×10^6 atoms. The system was allowed to relax under the constant number, pressure and temperature (NPT) ensemble for 50 ps at a desired temperature. The results of the temperature-

dependent density shown in Fig. 3(b) are in a good agreement with each other.

Simulated cases

The snapshots of the single molten drop impact onto the aluminum plate for three different impact speeds are shown in Fig. 4. Similarly, the successive impacts of two molten aluminum drops are shown in Fig. 5.

From the results in Figs. 4 and 5, the height and width of the fully solidified drop on the substrate decreased and increased, respectively, as the impact speed increased.

The variations of the height and width are shown in Fig. 6(a) and (b) for the single and double solidified drops, respectively. The results from EAM, MEAM and Comb3FF potentials were also compared. As the impact speed increases, the height of the fully solidified drop on the substrate decreases. For example, when the impact speed was doubled from 0.5 to 1.0 Å/ps, the heights of the fully solidified single and double drops decreased by factors of 1.14 and 1.16, respectively predicted using the EAM potential. For the same increase in the impact speed (0.5 to 1.0 Å/ps), the widths of the fully solidified single and double drops increased by factors of 1.10 and 1.11, respectively predicted using the EAM potential. It is well-known that predictions from classical MD simulations strongly depend on the appropriate choice of interatomic potential in describing the atomic interactions. From the obtained results shown in Fig. 6(a) and (b), the heights for single and double drop cases predicted using three different potentials showed some deviations. The results predicted using MEAM and Comb3FF were closer to each other when compared to EAM results, though the differences were not very significant. Since MEAM and Comb3FF potentials were more elaborated compared to EAM, such deviations could be expected. For example, the Comb3FF potential was a variable charge potential and the electronegativity equalization method was used to calculate the equilibrium change on each atom in the system, which was rather different from a less elaborated potential such as EAM. However, differences in the predicted widths of single and double drop cases using the three different potentials were insignificant.

The depth to which the molten drop penetrated the substrate (penetration depth) during the initial impact of the single drop was obtained for three different impact speeds as shown in Fig. 7(a), using three different potentials (EAM, MEAM and Comb3FF). Interestingly, the results and the trends obtained using these three different potentials were very close to one another. Considering the results from using the EAM potential, the penetration depth increased by factors of 1.40 and 1.43 when the impact speed increased from 0.5 to 1.0 Å/ps and from 1.0 to 2.0 Å/ps, respectively. The penetration depth for the double molten drop case was obtained when the first drop fully solidified on the substrate (see Fig. 7b). Similarly, the results obtained using the
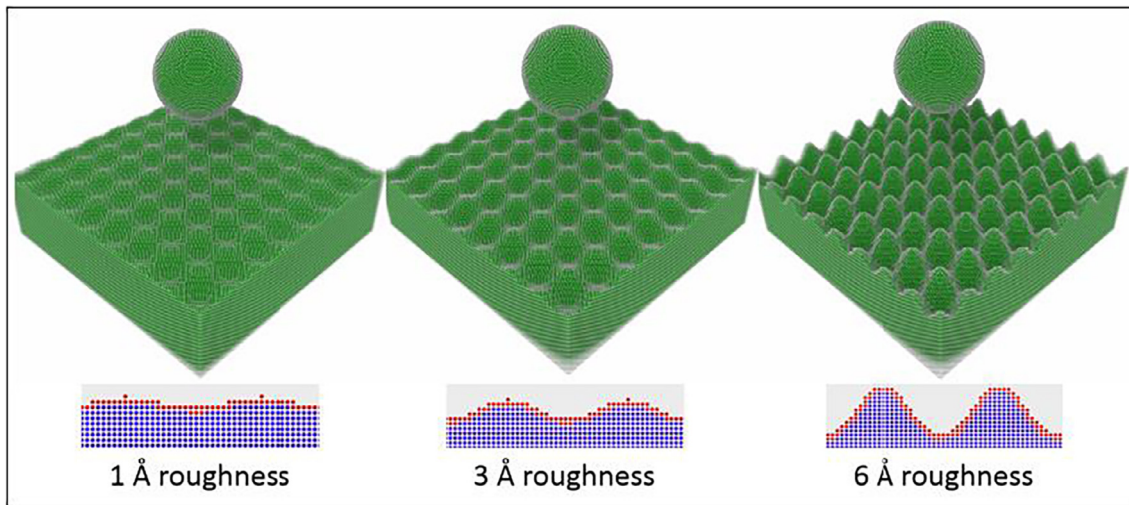
Fig. 2. Three-dimensional snapshots showing the surface topology of aluminum plates with three different roughness values.
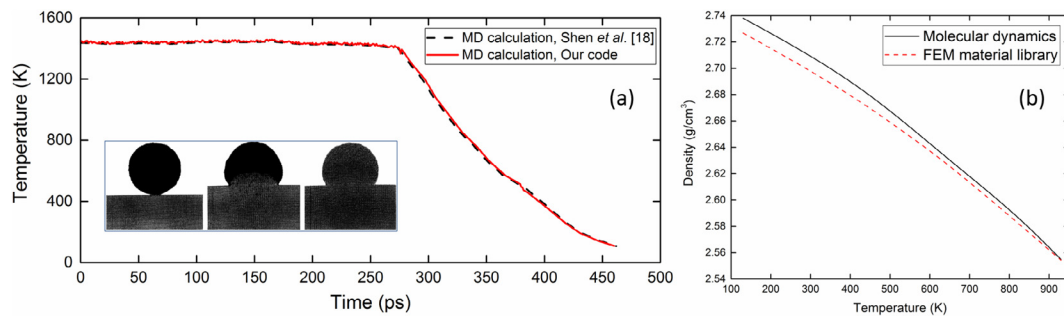

Fig. 3. (a) Comparisons between variations in temperature of gold molten drop upon impact onto a gold substrate from Shen et al. [18] and from our code. The inset shows snapshots of impact and solidification the molten drop and (b) variations in the temperature-dependent density of aluminum from our code and those obtained from the FEM material library.
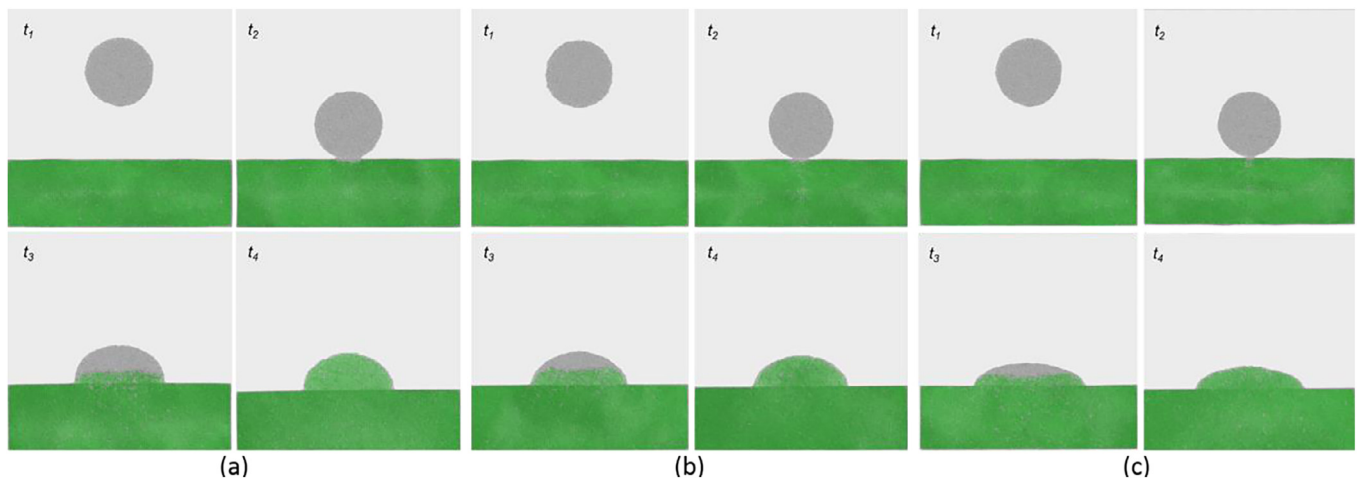

Fig. 4. Impact of single molten aluminum drop onto a solid aluminum plate at (a) 0.5, (b) 1.0 and (c) 2.0 Å/ps speed. (t_1: the initial position of molten drop, t_2: molten drop before impact, t_3: solidification of half of the molten drop and t_4: full solidification). (Grey color represents molten aluminum drop and green color represents the solid aluminum plate). (For interpretation of the references to color in this figure legend, the reader is referred to the web version of this article.)

three different potentials were not significantly different from one another. The penetration depth increased by a factor of 1.57 when the impact speed increased from 0.5 to 1.0 Å/ps. However, this factor decreased to 1.36 when the impact speed further increased from 1.0 to 2.0 Å/ps, which was attributed to the reduction in the local penetration efficiency as a result of the impact of the more flattened molten drop on the curved surface of the previous already fully solidified drop. Similar to the findings by Li et al. [12], we noted the simultaneous

solidification of the molten aluminum drops as a result of heat transfer to the substrate.

The depths to which the molten drop penetrated the substrate (penetration depth) during the initial impact of the single drop were obtained for three different impact speeds as shown in Fig. 8, using three different surface roughness values. The penetration depth was measured as the molten depth in the aluminum substrate which was located
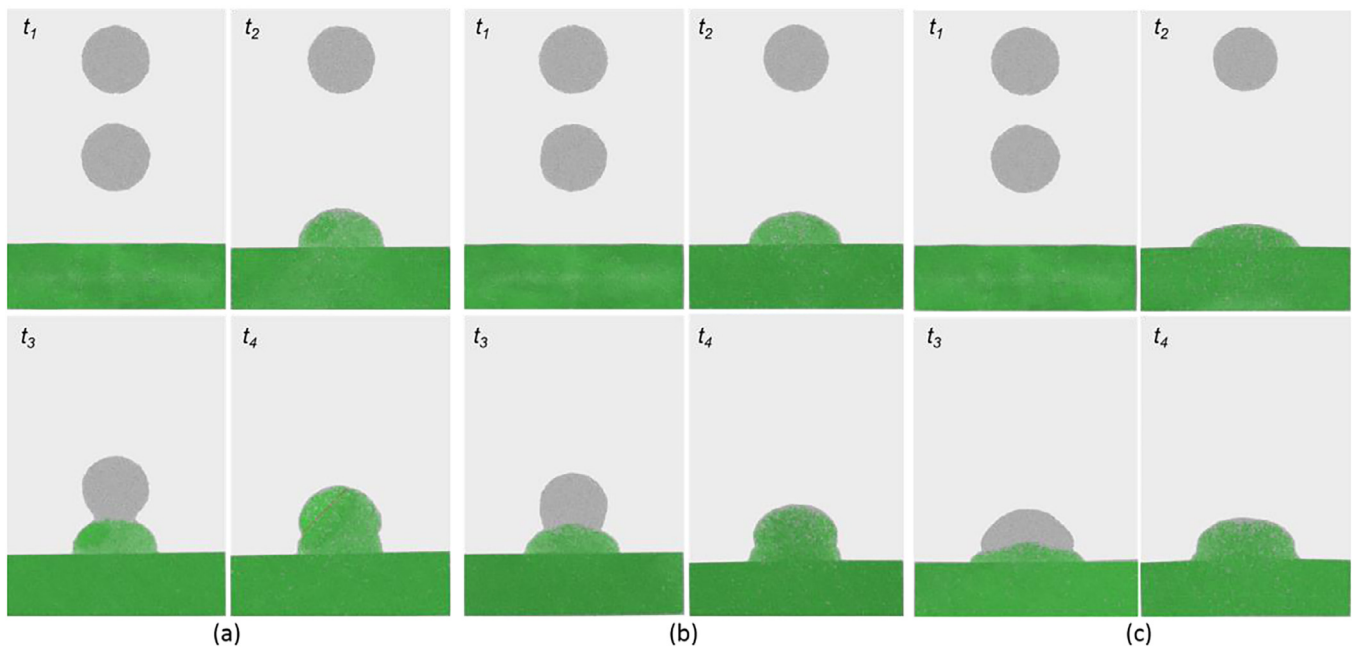
Fig. 5. Impact of double molten aluminum drops onto a solid aluminum plate at (a) 0.5, (b) 1.0 and (c) 2.0 Å/ps speed. (t_1: the initial position of molten drops, t_2: impact and solidification of first molten drop, t_3: impact of second molten drop, and t_4: full solidification). (Grey color represents molten aluminum drop and green color represents the solid aluminum plate). (For interpretation of the references to color in this figure legend, the reader is referred to the web version of this article.)
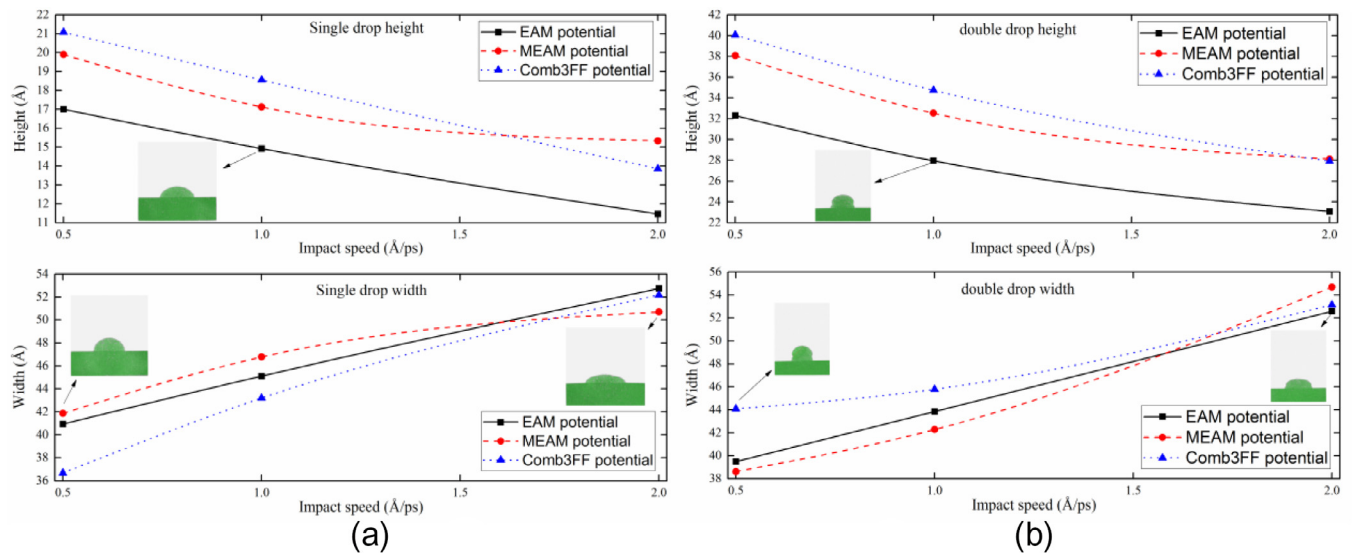

Fig. 6. Variation of the height and width of the solidified (a) single and (b) double drops on the substrate using three different potentials.

below the generated surface roughness. For the case with larger roughness peaks, the penetration depth in the substrate was found to be lower when compared to the case with finer roughness. The large roughness peaks acted as impediment to the path of the molten drop to interact with the substrate underneath and therefore the penetration depth during the initial impact of the single drop in the substrate would be reduced. On the contrary, the molten drop that impacted a flat surface (or a surface with finer roughness) could transfer its energy directly to the atoms of the substrate and thus created a larger penetration depth in the substrate.

The variations of the maximum molten height versus time were determined for the two different cases shown in this paper (i.e., single and double drop cases). For the single drop case, the molten height was determined from the time when the molten drop touched the surface of the aluminum plate; for the double drop case, it was measured when the

second molten drop touched the curved surface of the first fully solidified drop. The results are shown in Fig. 9(a) and (b) for single and double drop cases, respectively.

The molten height decreased with time for both cases, due to heat transfer from the molten drop to the underneath surface at a temperature lower than that of the molten drop. Moreover, the molten height for the single drop case decreased more quickly upon impacting the aluminum plate (see Fig. 9a), when compared to the height for the double drop case upon the molten drop impacting the curved surface of the first fully solidified drop (see Fig. 9b). The flat surface of the aluminum plate was more efficient in cooling the molten drop due to the larger surface area taken up by the molten drop upon its impact. The maximum molten height decreased at a faster rate for higher impact speeds due to the more effective flattening of the molten drop and thus taking up a larger surface area upon impact, and in turn the further
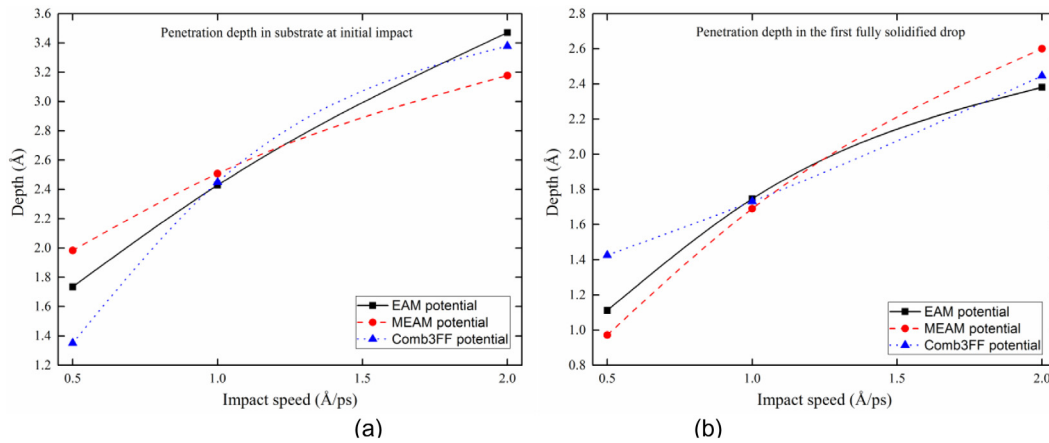
Fig. 7. Penetration depth of the molten drop on (a) substrate and (b) first fully solidified drop using three different potentials.
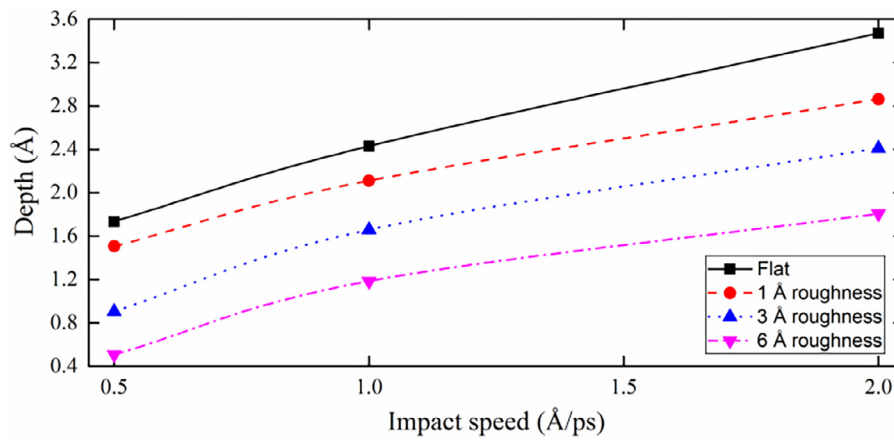

Fig. 8. Penetration depths of the molten drop upon initial impact onto the aluminum substrate with different surface roughness. (Note: the penetration depth was measured when the molten drop impacted the substrate underneath the surface roughness).
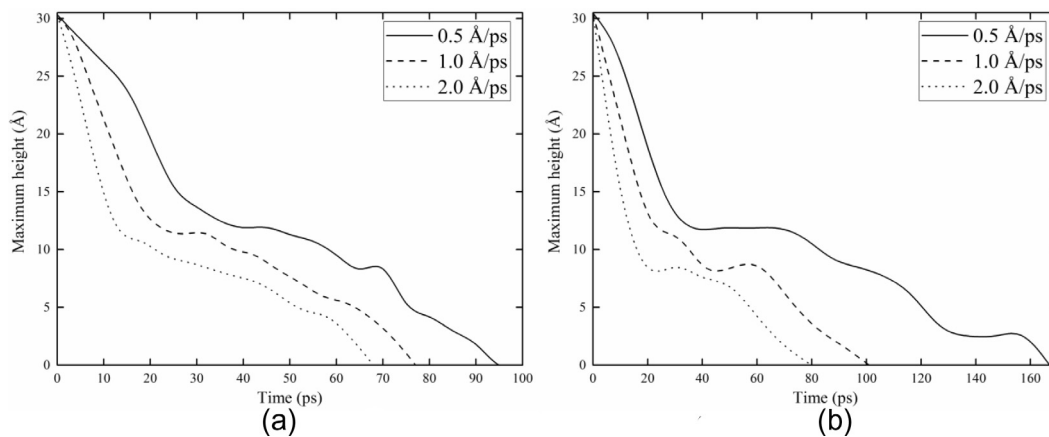

Fig. 9. Maximum molten drop height versus time for (a) single and (b) double drop cases for different impact speeds.

enhanced heat transfer. Similar observations were made in the previous work of Shen et al. [18] who showed that the temperature of a single gold molten drop on the substrate decreased at a faster rate for higher impact speeds. Lastly, for metallic systems, there are known order parameters that enable the specification of local order in the system [19,20]. For the present metallic system, the finally impacted droplet on the aluminum plate that was allowed to fully solidify was found to have an FCC structure. Similar observation was made in the previous work of Shen et al. [18].

Conclusions

The present work focused on modeling the pileup process at the atomic scale using molecular dynamics. We considered two different setups, namely, (1) single and (2) double molten aluminum drop impact onto a solid aluminum substrate. Most previous investigations employed the widely used continuum scale Volume-of-Fluid (VOF) method to model the pileup phenomena. The underlying mechanism of the pileup process could be studied in more details through modeling at the atomic scale. The final solidified structure could also be assessed in

terms of defect and crystallinity. The present model would be a useful tool for future investigators, hopefully to tackle issues related to poor metallurgical properties of the final structure. Nevertheless, it is remarked that the MD method requires large computational resources since atomistic models are known to be computationally expensive.

References

[1] Attinger D, Zhao Z, Poulikakos D. An experimental study of molten microdroplet surface deposition and solidification: transient behavior and wetting angle dynamics. J Heat Transf 2000;122:544–56.

[2] Pasandideh-Fard M, Chandra S, Mostaghimi J. A three-dimensional model of droplet impact and solidification. Int J Heat Mass Transf 2002;45:2229–42.

[3] Haferl S, Poulikakos D. Experimental investigation of the transient impact fluid dynamics and solidification of a molten microdroplet pile-up. Int J Heat Mass Transf 2003;46:535–50.

[4] Le Bot C, Vincent S, Arquis E. Impact and solidification of indium droplets on a cold substrate. Int J Therm Sci 2005;44:219–33.

[5] Yarin AL. Drop impact dynamics: splashing, spreading, receding, bouncing. Annu Rev Fluid Mech 2006;38:159–92.

[6] Vincent S, Le Bot C, Sarret F, Meillot E, Caltagirone JP, Bianchi L. Penalty and eulerian–lagrangian VOF methods for impact and solidification of metal droplets plasma spray process. Comput Fluids 2015;113:32–41.

[7] Du J, Wei Z, Chen Z, Li S, Tang Y. Numerical investigation of pileup process in metal microdroplet deposition manufacture. Micromachines 2014;5:1429–44.

[8] Wang CH, Tsai HL, Hwang WS. Direct printing of 1-D and 2-D electronically conductive structures by molten lead-free solder. Materials 2016;10:1.

[9] Tsai MH, Hwang WS, Chou HH. The micro-droplet behavior of a molten lead-free solder in an inkjet printing process. J Micromech Microeng 2009;19:125021.

[10] Son HY, Nah JW, Paik KW. Formation of Pb/63Sn solder bumps using a solder droplet jetting method. IEEE Trans Electron Packag Manuf 2005;28:274–81.

[11] Tian DW, Wang CQ, Tian YH. Effect of solidification on solder bump formation in solder jet process: Simulation and experiment. Trans Nonferrous Metals Soc China 2008;18:1201–8.

[12] Li H, Wang P, Qi L, Zuo H, Zhong S, Hou X. 3D numerical simulation of successive deposition of uniform molten Al droplets on a moving substrate and experimental validation. Comput Mater Sci 2012;65:291–301.

[13] Zhou XW, Wadley HN, Johnson RA, Larson DJ, Tabat N, Cerezo A, et al. Atomic scale structure of sputtered metal multilayers. Acta Mater 2001;49:4005–15.

[14] Lenosky TJ, Sadigh B, Alonso E, Bulatov VV, de la Rubia TD, Kim J, et al. Highly optimized empirical potential model of silicon. Modell Simul Mater Sci Eng 2000;8:825.

[15] Liang T, Shan TR, Cheng YT, Devine BD, Noordhoek M, Li Y, et al. Classical atomistic simulations of surfaces and heterogeneous interfaces with the charge-optimized many body (COMB) potentials. Mater Sci Eng R: Reports 2013;74:255–79.

[16] Choudhary K, Liang T, Chernatynskiy A, Lu Z, Goyal A, Phillpot SR, et al. Charge optimized many-body potential for aluminum. J Phys: Condens Matter 2014;27:015003.

[17] Hünenberger PH. Thermostat algorithms for molecular dynamics simulations. Advanced computer simulation. Springer; 2005. p. 105–49.

[18] Shen D, Zou G, Liu L, Wu A, Duley WW, Zhou YN. Investigation of impact and spreading of molten nanosized gold droplets on solid surfaces. Appl Opt 2018;57:2080–6.

[19] Eslami H, Khanjari N, Müller-Plathe F. A local order parameter-based method for simulation of free energy barriers in crystal nucleation. J Chem Theory Comput 2017;13:1307–16.

[20] Eslami H, Sedaghat P, Müller-Plathe F. Local bond order parameters for accurate determination of crystal structures in two and three dimensions. PCCP 2018;20:27059–68.